

⁴L. Onsager, Phys. Rev. **65**, 117 (1944).

⁵J. R. Fontaine and C. Gruber, Commun. Math. Phys. **70**, 243 (1979).

⁶B. McCoy and T. T. Wu, *The Two Dimensional Ising Model* (Harvard Univ. Press, Cambridge, Mass., 1973).

⁷J. L. Lebowitz, J. Statist. Phys. **16**, 463 (1977), and in *Mathematical Problems in Theoretical Physics*, ed-

ited by G. Dell'Antonio, S. Doplicher, and G. Jona-Lasinio, Lecture Notes in Physics Vol. 80 (Springer, Berlin, 1978), p. 68.

⁸M. J. de Oliveira, D. Furman, and R. B. Griffiths, Phys. Rev. Lett. **40**, 977 (1978).

⁹Compare C. Itzykson, M. E. Peskin, and J. B. Zuber, Phys. Lett. **95B**, 259 (1980).

New Models for Metal-Induced Reconstructions on Si(111)

G. V. Hansson,^(a) R. Z. Bachrach, and R. S. Bauer
Xerox Palo Alto Research Center, Palo Alto, California 94304

and

P. Chiaradia^(b)

Stanford Synchrotron Radiation Laboratory, Stanford, California 94305
(Received 2 September 1980)

Angle-resolved photoelectron spectroscopy and surface-core-level chemical shifts have been used to study electronic structure and derive structural models of the Al, Ag, and Ni metal-induced reconstructions on Si(111). We show, for the first time, the connection between the Ni-stabilized $\sqrt{19} \times \sqrt{19}$ and clean 7×7 surfaces, and report a new Si(111)- $(\sqrt{7} \times \sqrt{7})$ Al structure at < 0.5 monolayer coverage of Al.

PACS numbers: 73.20.Hb, 73.40.Ns, 79.60.Gs

The origin of the surface reconstructions on the Si(111) surface have been of active interest for some time.^{1,2} The interaction between silicon and initial metal overlayers has also been the subject of many studies with low-energy electron-diffraction (LEED), electron energy-loss, Auger, and photoelectron spectroscopies,^{3,4} but a full understanding of the reconstructions and surface electronic states has not been obtained.⁵

New results are presented in this paper which provide insight into metal-silicon surface structures from angle-resolved valence-band photoemission and surface-core-level chemical-shift measurements carried out on ordered metal-silicon systems where the number of metal atoms ranges from < 0.1 monolayer Ni to 0.5 monolayer Al to 1.0 monolayer Ag. We show the similarity of the electronic states for the $(\sqrt{19} \times \sqrt{19})$ Ni and 7×7 reconstructions and present for the first time a model which relates the two. By using the angular dependence of the emission as well as the energy dispersion of the metal-silicon bands we derive structural models for the $(\sqrt{3} \times \sqrt{3})$ Al and $(\sqrt{3} \times \sqrt{3})$ Ag and the new $(\sqrt{7} \times \sqrt{7})$ Al surface structures on Si(111).

The metal-silicon structures have been prepared by evaporating controlled amounts of metal

onto clean room-temperature Si(111) 7×7 surfaces. This generally results in a metal-covered surface that shows a 7×7 reconstruction, but does not necessarily correspond to an ordered metal overlayer. To obtain the ordered metal-silicon reconstructions, the surfaces have to be annealed. Typically the change to an ordered phase is accompanied by a change in surface chemical shifts. For example, for the Al $2p$ at submonolayer coverages on Si(111), a binding energy 0.15 eV higher than the metallic core line is obtained. When the surface reconstructs to either the $\sqrt{3} \times \sqrt{3}$ or the $\sqrt{7} \times \sqrt{7}$, the shift to higher binding energy further increases to 0.35 eV. The line shape broadens by 15% with respect to the metallic core line because of the Si-Al bond. We have also studied the characteristic surface-core-level line shapes and shifts of the Si(111) $2p$ for the 2×1 and 7×7 surfaces^{6,7} in the course of this work and this will be reported elsewhere.

We discuss first the Si(111) $\sqrt{19} \times \sqrt{19}$, which is often obtained as an unintentional impurity-stabilized surface⁸ after long annealings at quite high temperatures (1000–1200 °C). The Auger spectra always show some amount of impurity Ni. We also have found that, under some circumstances, such high-temperature annealing can produce cop-

per contamination which results in features reported to be due to silicon surface states.⁹ All the results reported here eliminated these problems.

To determine the concentration of Ni atoms needed to get a good $\sqrt{19} \times \sqrt{19}$ structure, controlled amounts of Ni were evaporated from an electroplated tungsten filament. The surface was exposed to Ni flux for typically 20 sec with a constant evaporation rate of 0.005 M.L./sec (1 M.L. = 1 monolayer) established with a thickness monitor. The surfaces were then annealed at 800 °C. At this temperature the uncontrolled diffusion of impurity Ni to the surface was not observed. We find that excellent $\sqrt{19} \times \sqrt{19}$ LEED patterns can be obtained with 0.08 ± 0.03 M.L. of Ni. This rules out the possibility that the surface is a reconstruction involving a monolayer of silicide. Rather, the unit cell of 19 Si-lattice sites contains only one Ni atom.

Figure 1 compares the photoemission from the clean 2×1 and 7×7 surfaces¹⁰ with that from the

$\sqrt{19} \times \sqrt{19}$ impurity-stabilized surface. (An impurity-stabilized structure is defined as one where a minority of the silicon surface atoms interact directly with the metal atoms.) The data were obtained at the Stanford Synchrotron Radiation Laboratory with use of a new multidetection angle-resolved spectrometer.¹¹

Figure 1(a) shows the photoemission in the normal direction for 22 eV excitation which was emphasized because the cross section from the dangling bond on the clean 2×1 surface has a local maximum. Figure 1(b) shows the angle-resolved photoemission measured in the off-normal directions for the 7×7 and $(\sqrt{19} \times \sqrt{19})$ Ni surfaces. The similarity between the spectra suggests that the two reconstructions are quite similar.

The dangling-bond emission marked by arrows can be identified as structures near the valence-band maximum on all three surfaces. The intensities of the structures are very sensitive to oxygen contamination and the polarization of the light. To excite these dangling-bond states the

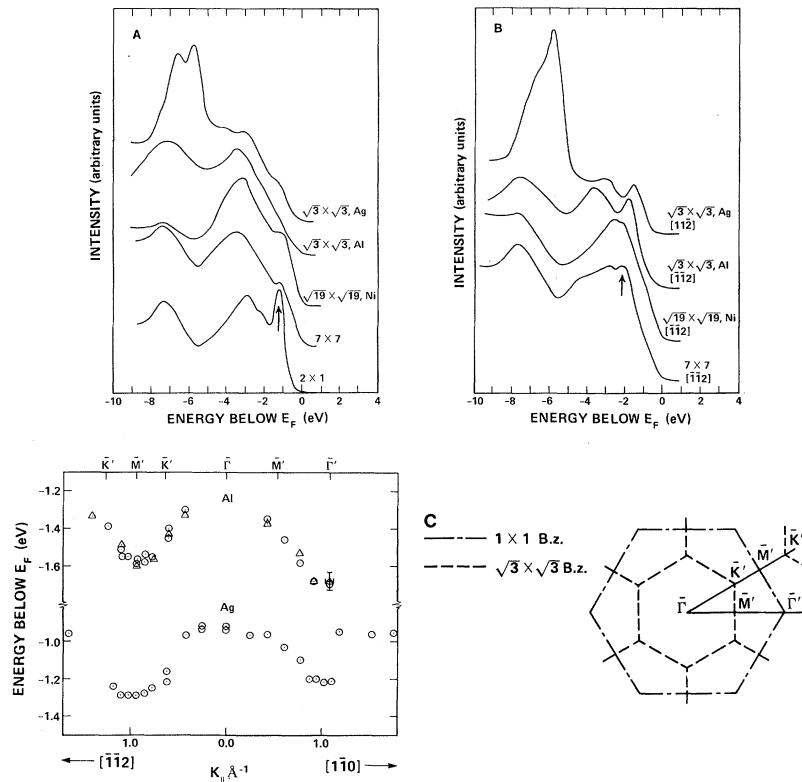


FIG. 1. Normal-emission and various polar and azimuthal spectra from the various Si(111) surfaces selected to emphasize the physics discussed in this paper. $\hbar\omega = 22.0$ eV; p polarized; $\theta_i = 45^\circ$. (a) $\theta_d = 0^\circ$. (b) $\theta_d = 27^\circ$. (c) The dispersion for the extrinsic-state emission for the $(\sqrt{3} \times \sqrt{3})$ Al and $(\sqrt{3} \times \sqrt{3})$ Ag surfaces derived from the full range of data as a function of angle.

light has to have a component of A normal to the surface. The dangling bond is a sharp feature for the 2×1 and has a strong dispersion (0.6 eV) in some directions of \vec{k} space, while for the 7×7 and $\sqrt{19} \times \sqrt{19}$ surfaces all the emission is broader. The photoemission reaches up to the Fermi level for the 7×7 surface indicating a metallic surface, while this is not conclusive for the $\sqrt{19} \times \sqrt{19}$ surface.

The new model we propose for the $\sqrt{19} \times \sqrt{19}$ impurity-stabilized surface is shown in Fig. 2 and is derived from the smooth 7×7 reconstruction model¹ previously obtained with the energy-minimization technique which showed that ringlike structures of up and down atoms are energetically favorable. We propose that the raised three-atom "ring" is surrounded by nine down atoms followed by fifteen up atoms. The resulting up-down pattern shown in Fig. 2 has ten up and nine down atoms, which is close to the 50/50 ratio expected from the lowered atoms to the raised atoms as in the 2×1 and 7×7 reconstructions of the clean surface. In this $\sqrt{19} \times \sqrt{19}$ model, the Ni atoms sit in the hollow position between the first two Si layers, and, with respect to the silicide, the atoms above and below are missing in the six-fold site. The Ni-Si distance for this position is very close to the value in the silicide where the lattice parameter of the silicide (5.406 Å) is an excellent match to that of silicon (5.428 Å). Since the silicide, NiSi₂, is known to grow epitaxially on Si(111) at the annealing temperatures used,^{12, 13} it is reasonable that the geometric configuration for the Ni atoms on the $\sqrt{19} \times \sqrt{19}$ surface is similar to the silicide structure. To make the geometry even more similar to the silicide configuration, the three Si atoms in the top layer would be raised and the three second-layer atoms lowered.

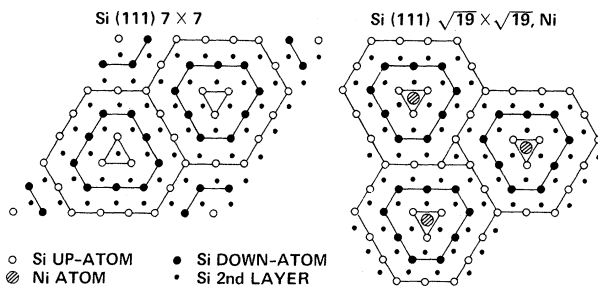


FIG. 2. Proposed model for the nickel-impurity-stabilized $\sqrt{19} \times \sqrt{19}$ surface based upon the buckled ring concept for the 7×7 surface. Note that this surface is a precursor of the Ni silicide formation.

Al and Ag behave differently than Ni and new surface structures have only been obtained at high enough metal coverages that all surface silicon atoms are bonded to metal atoms. We find that the $(\sqrt{3} \times \sqrt{2})$ Al arises at $\frac{1}{3}$ monolayer coverage and the $(\sqrt{7} \times \sqrt{7})$ Al surface, which has not been reported before, arises at 0.5 monolayer coverage. The $(\sqrt{3} \times \sqrt{3})$ Ag arises at 1 monolayer coverage and thus it is structurally different although it has the same size unit cell as $(\sqrt{3} \times \sqrt{3})$ Al.

For the $\sqrt{3} \times \sqrt{3}$ and $\sqrt{7} \times \sqrt{7}$ metal overlayers of Al, there is no detectable dangling-bond emission in the normal direction. The normal emission from the $(\sqrt{3} \times \sqrt{3})$ Ag surface is dominated by two peaks from the $4d$ states of Ag at -5.7 and -6.6 eV. The center of gravity of this emission is 0.8 eV lower than the emission from the Γ point in bulk silver.¹⁴ This shift of $4d$ states can be explained by the induced dipole due to the charge transfer from the hybridized $5s$ states around the silver atoms to the bonding orbitals between silver and silicon atoms.

Comparing the emission from all the surfaces, we find the 7×7 surface has the strongest emission close to the Fermi level, i.e., stronger metallic character than the metal-covered surfaces. In the energy region where the dangling bond occurs for the clean surface, we see only a weak shoulder on the metal-silicon surfaces. One would expect the dangling bond to be changed by some orbital bonding to the metal atoms.

The polar- and azimuthal-angle dependences of the photoemission from the new states that replace the dangling bond on the Al and Ag overlayer structures have been studied. In Fig. 1(b), we show examples where these states are strong and for reference we also show a 7×7 spectrum where the low-energy (-2 eV) surface state is seen. The emission from this state on the clean surface has a threefold symmetry, peaking towards the $[112]$ direction. We interpret it as a backbond state, since it does not have the p_x , s character of the dangling bond.

For the aluminum overlayer surfaces we find a new state around -1.7 eV, i.e., intermediate in energy between the dangling bond and the back bond for the clean surface. The extrinsic-state emission has a strong azimuthal- and polar-angle dependence. For p -polarized light with $\theta_i = 45^\circ$, we find the maximum intensity at 25° polar angle with \vec{k}_{\parallel} in the $[112]$ direction (threefold symmetric). Strong similarity with the emission pattern from the backbond state on clean Si(111) 7×7 with nearly the same final-state energy indicates that

the final-state scattering is similar in the two cases. This is consistent with the aluminum atoms in the threefold hollow site, but *not* on the threefold site with a second-layer silicon atom below. Figure 3 shows the reconstruction models that we have deduced which show this site.

For the silver overlayer surface, an extrinsic state at -1.4 eV arises that has a maximum emission at 25° polar angle. The threefold azimuthal dependence is, however, *opposite* to that for the $(\sqrt{3}\times\sqrt{3})$ Al surface with the maximum intensity for \vec{k}_\parallel in the $[112]$ direction. This means that the bonding direction is opposite for the two overlayer structures, as can be seen in the models presented in Fig. 3. We conclude from this result that the three Ag atoms in an earlier proposed model¹⁵ are centered above the second-layer Si atom (Fig. 3).

The experimental dispersion obtained from the angle-resolved photoemission for the extrinsic state on the Si(111)- $(\sqrt{3}\times\sqrt{3})$ Al surface (inset in Fig. 1) shows that the dispersion is symmetric around a minimum at M' in the $\Gamma K'M'K'$ direction. (Primed letters indicate high-symmetry points in the $\sqrt{3}\times\sqrt{3}$ surface Brillouin zone.) The absolute minimum of the dispersion is at the outer Γ' point in the $\Gamma M'\Gamma'$ direction. It is interesting to note that the shape of the dispersion with respect to the 1×1 surface Brillouin zone is the same as has been calculated for the dangling-bond band of the ideal clean 1×1 surface.¹⁶

We propose that the extrinsic state on the Si(111)- $(\sqrt{3}\times\sqrt{3})$ Al surface has enough character of the dangling bond so that the similarity in dispersion is not accidental. The effect of the Al overlayer is twofold. First, it makes the surface unit cell three times larger than for the 1×1 surface, which means that the dangling-bond band

will correspond to three bands in the surface $\sqrt{3}\times\sqrt{3}$ Brillouin zone. Secondly, the Al atoms bring one $3p$ electron per unit cell that is close enough in energy to interact with the dangling-bond electrons. We thus end up with four electrons per unit cell that can fill two of the three dangling-bond-derived bands. The experiment shows that there are two occupied bands, since the measured dispersion gives different energy values for states at two different M' points, which are equivalent points in the $\sqrt{3}\times\sqrt{3}$ surface Brillouin zone. Since the width of the peak is relatively large (full width at half maximum = 0.7 eV), compared with the dispersion 0.3 eV, we have not been able to resolve the two bands in any spectra.

Our experiments show that the aluminum atoms contribute electrons to the extrinsic surface state since we find an increased intensity with increasing Al coverage. Based on the similarity in electronic structure of the $\sqrt{7}\times\sqrt{7}$ surface with the $\sqrt{3}\times\sqrt{3}$ surface as well as the determined value of ≤ 0.5 M.L. Al coverage, we have constructed a model for the $\sqrt{7}\times\sqrt{7}$ structure shown in Fig. 3 in which both the $\sqrt{3}\times\sqrt{3}$ and $\sqrt{7}\times\sqrt{7}$ models satisfy the criterion that there is an even number of electrons per unit cell that can contribute to the high-energy surface state, i.e., counting the dangling-bond electrons on Si plus the $3p$ electrons on the Al atoms.

The energy dispersion of the extrinsic surface state on the Si(111)- $(\sqrt{3}\times\sqrt{3})$ Ag surface shown in the inset in Fig. 1 is similar to the Al-covered surface and it is at ≈ 0.3 eV higher energy. We find the peak position at equivalent M' points to be at different energies showing that there is more than one occupied band in the $\sqrt{3}\times\sqrt{3}$ Brillouin zone for this surface.

The authors acknowledge useful conversations with Dr. D. J. Chadi and Dr. R. H. Williams. Some of the materials incorporated in this work were developed at the Stanford Synchrotron Radiation Laboratory, which is supported by the National Science Foundation under Grant No. DMR-77-27489 in cooperation with the Stanford Linear Accelerator Center and the U. S. Department of Energy.

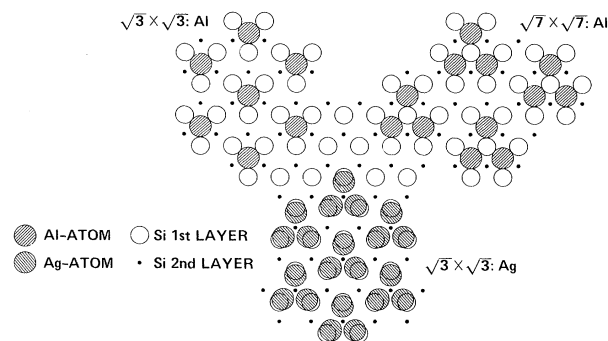


FIG. 3. Structural models proposed for Al- and Ag-metal-induced surface reconstructions discussed in the text.

^(a)Present address: Department of Physics and Measurement Technology, Linköping University, S-58183 Linköping, Sweden.

^(b)Present address: Istituto di Fisica G. Marconi, Università degli Studi di Roma, Piazza A Moro 5, I-

00185 Roma, Italy.

¹D. J. Chadi, R. S. Bauer, R. H. Williams, G. V. Hansson, R. Z. Bachrach, J. M. Mikkelsen, Jr., F. Houzay, G. M. Guichard, R. Pinchaux, and Y. Pétroff, *Phys. Rev. Lett.* **44**, 799 (1980).

²J. C. Phillips, *Phys. Rev. Lett.* **45**, 905 (1980).

³J. J. Lander and J. Morrison, *J. Appl. Phys.* **36**, 1706 (1965).

⁴J. E. Rowe, G. Margaritondo, and S. B. Christman, *Phys. Rev. B* **15**, 2195 (1977).

⁵H. I. Zhang and M. Schlüter, *Phys. Rev. B* **18**, 1923 (1978).

⁶F. J. Himpsel, P. Heimann, T.-C. Chiang, and D. E. Eastman, *Phys. Rev. Lett.* **45**, 1112 (1980).

⁷S. Brennan, J. Stohr, R. Jaeger, and J. E. Rowe, *Phys. Rev. Lett.* **45**, 1414 (1980).

⁸A. J. van Bommel and F. Meyer, *Surf. Sci.* **8**, 467 (1967).

⁹M. C. Muñoz, V. Martínez, J. A. Tagle, and J. L.

Sacedón, *Phys. Rev. Lett.* **44**, 814 (1980).

¹⁰G. V. Hansson, R. Z. Bachrach, R. S. Bauer, D. J. Chadi, and W. Gopel, *Surf. Sci.* **99**, 13 (1980).

¹¹G. V. Hansson, B. Goldberg, and R. Z. Bachrach, *Rev. Sci. Instrum.*, to be published.

¹²J. C. Bean, J. M. Poate and K. C. R. Chiu, *Electronic Materials Conf.* (1980).

¹³N. W. Cheung, R. J. Culbertson, L. C. Feldman, P. J. Silverman, K. W. West, and J. W. Mayer, *Phys. Rev. Lett.* **45**, 120 (1980).

¹⁴R. F. Davis, K. A. Mills, G. Thornton, S. D. Kevan, and D. A. Shirley, in *Proceedings of the Sixth International Conference on Vacuum Ultraviolet Radiation Physics*, Charlottesville, Virginia, 1980 (to be published).

¹⁵F. Wehking, H. Beckerman, and R. N. Niedermayer, *Surf. Sci.* **71**, 364 (1978).

¹⁶K. C. Pandey and J. C. Phillips, *Phys. Rev. Lett.* **32**, 1433 (1974).